ELSEVIER

Applied Mathematical Modelling 26 (2002) 377–396

APPLIED MATHEMATICAL MODELLING

www.elsevier.com/locate/apm

On coupling electromagnetic fields and lumped circuits with TLM

A.J. Mariani, S.M. Kirkup *, Y. Huang, G.R. Jones

Department of Electrical Engineering and Electronics, University of Liverpool, Brownlow Hill, Liverpool L69 3GJ, UK

Received 3 June 2000; accepted 4 May 2001

Abstract

The application of the transmission-line matrix (TLM) method to the modelling of the evolving electromagnetic field within a capacitor structure is considered in this paper. The experiment of Al-Asadi et al. [Electron. Lett. 30 (4) (1994)], consisting of the capacitor connected to a source and a resistor and modelling the current following an abrupt switch-on, is reconsidered. The effect of using finer TLM meshes and extending the mesh beyond the capacitor structure is studied. The outcome of replacing the abrupt switch-on by a smooth switch-on is also examined. The method employed in Al-Asadi et al. (loc. cite) for coupling the capacitor to the network, termed the *current sources method* is also used in this work. The practicalities of using this method and some of its effects are examined.

1. Introduction

Often the simulation of an electrical network involves *lumped* components, where a simple model of their behaviour is sufficient, and *distributed* components, where a detailed model of the electromagnetic field within a region is required. It is then necessary to couple the lumped and distributed components together in the overall model of the network. In this paper a simulation of a circuit containing lumped source and resistance components is coupled with a capacitor modelled as a distributive component.

The numerical method that is applied in this work is the *transmission-line modelling* method, otherwise known as the transmission-line matrix (TLM) method. It is a numerical technique for

* Corresponding author.
E-mail address: smk@electromagnetics.co.uk (S.M. Kirkup).

0307-904X/02/$ - see front matter
PII: S0307-904X(01)00043-9

simulating an electromagnetic field via an equivalent circuit model. The method is based on the equivalence between Maxwell's equations and the equations for voltages and currents on a mesh of two-wire transmission lines. A general description of the method is given in [3]. The TLM is a time-stepping method, similar to the better-known finite-difference time-domain (FD-TD) method [7] but derived in an entirely different manner. As with the FD-TD method, the TLM is generally applied in a truncated region of the full electromagnetic domain and a suitable boundary condition is used to model the region beyond this.

Recently, the TLM has been extended in order to simulate electric circuits involving the coupling of discrete and lumped components [1,2]. Results from the application of the TLM to the electromagnetic field within a capacitor of classical shape have recently been related in the paper by Al-Asadi et al. [1]. The purpose of the present paper is to extend the results of these reference papers and to appraise the TLM for this kind of application and the coupling method that has been proposed. The simulation of the transient current in the circuit containing a classical capacitor that is considered in these references is repeated, but with finer meshes and meshes that extend beyond the edge of the capacitor. The effect of a smoothed switch-on voltage is compared with the results from an abrupt switch-on.

The work covered in this paper results from the authors' interests in the simulation of circuit breakers [6] and in the modelling of the electromagnetic fields within real capacitors [4,5]. The methods employed in this paper have been written in the programming language Java and an interactive web page http://www.electromagnetics.co.uk/tlm.htm has been developed so that the reader may reconsider the test problems covered in this paper and easily experiment with alternative experimental conditions and with various meshes.

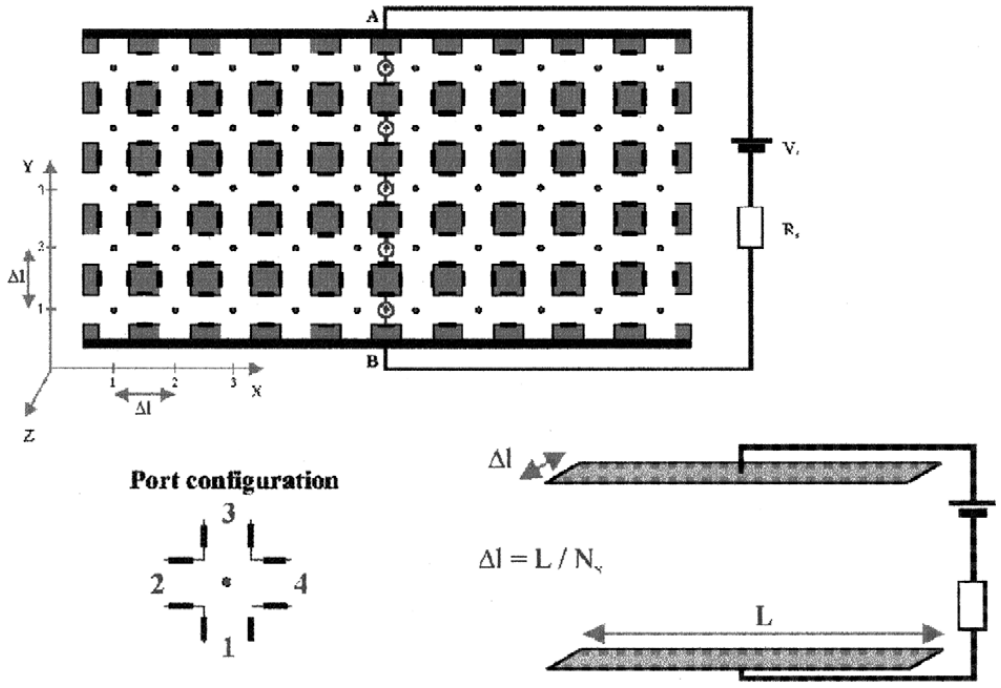

Fig. 1. The circuit, the 10×5 mesh and port configuration.

2. The circuit

To initiate this study, the TLM is to be applied to a similar circuit to the one in [1]. A capacitor lies in a circuit that is illustrated in Fig. 1 with the lumped components of a source voltage V_S and source resistance R_S. The capacitor is a parallel plate capacitor with plate width L (default = 10 mm) and distance d (= 5 mm) apart.

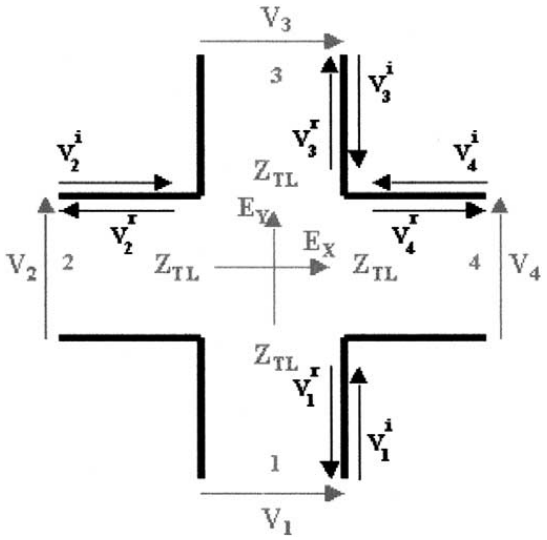

Fig. 2. The port configuration for each cell.

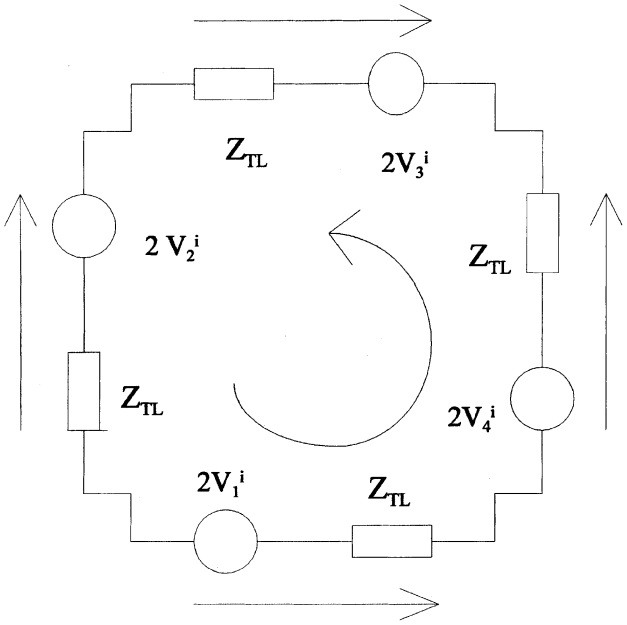

Fig. 3. The Thevenin equivalent circuit.

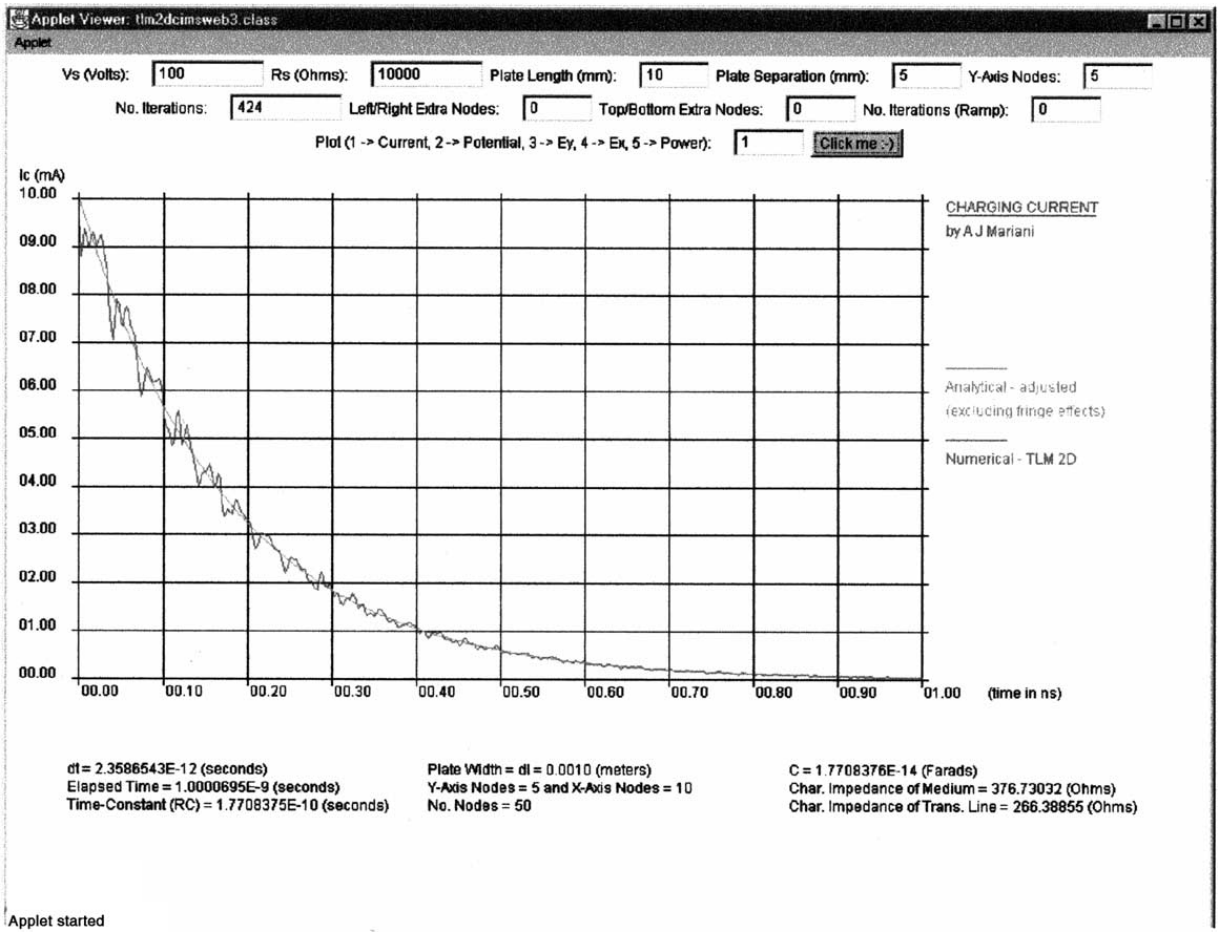

Fig. 4. Current in circuit for the 10×5 mesh.

The treatment of the capacitor as a distributed component requires a model of the electromagnetic field within and surrounding the plates. In Fig. 1, a typical TLM mesh within the capacitor plates is shown; the complete field being truncated with the region between the plates is replaced by an array of 1 mm $\times$ 1 mm cells, the remaining region being represented by a suitable choice of boundary condition for the mesh.

The charging profile of a classical parallel plate capacitor is well known. At a time t, after an abrupt switch-on, the potential difference across the capacitor is given by

$$V(t) = V_S\left(1 - \exp\left(\frac{-1}{R_S C}t\right)\right) \tag{1}$$

and the current in the circuit is given by

$$I(t) = \frac{V_S}{R_S}\exp\left(\frac{-1}{R_S C}t\right), \tag{2}$$

where C is the capacitance of the capacitor. The TLM approximations to the current in the circuit $I(t)$ following switch-on is considered in this paper.

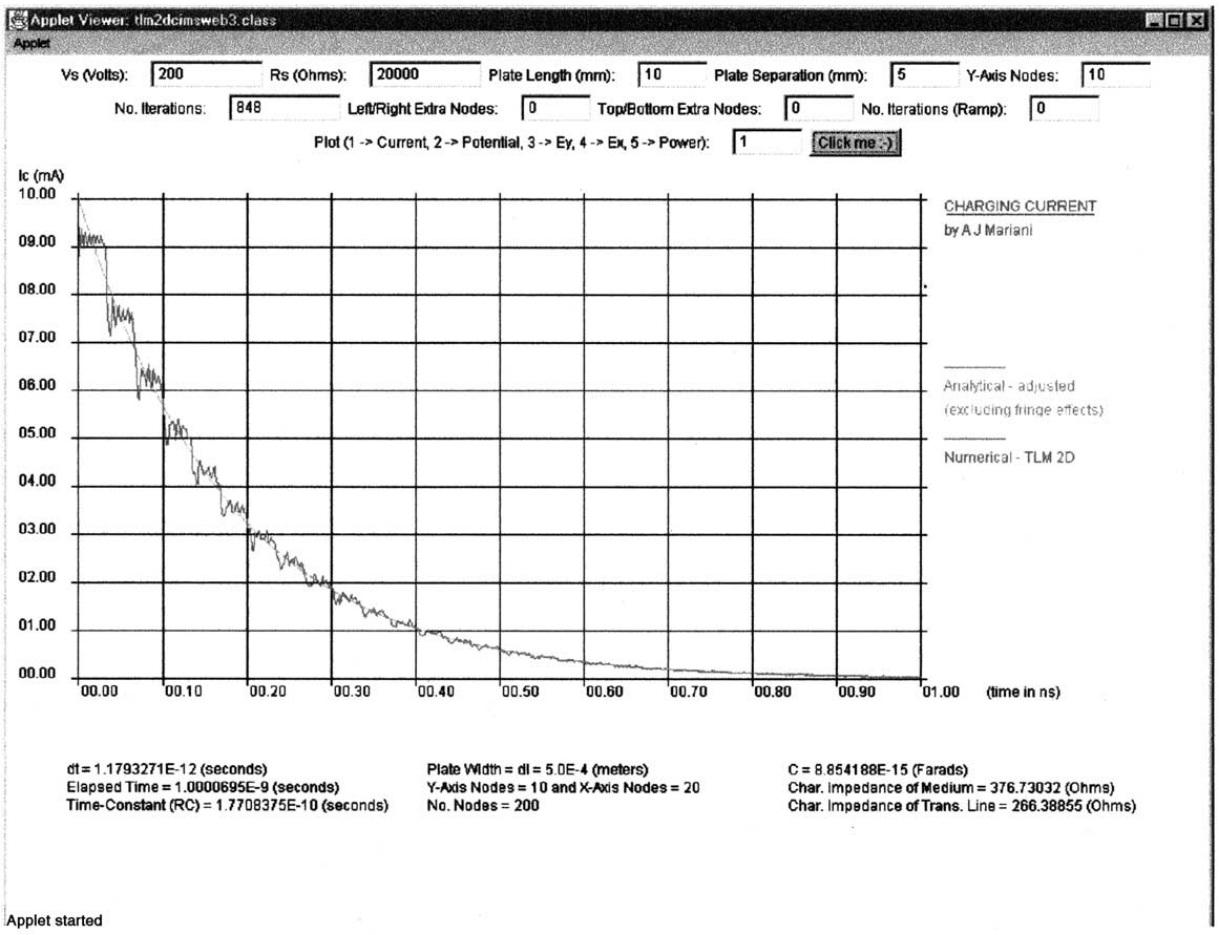

Fig. 5. Current in circuit for the 20×10 mesh.

3. TLM model

The capacitor is assumed to be a two-dimensional distributed field problem. Its discretisation into a system of 1 mm $\times$ 1 mm square cells as illustrated in Fig. 1. Results from this mesh and from finer meshes will be related later. In general let us assume that the cells are $\Delta l \times \Delta l$. The classical capacitor has capacitance $C = \epsilon(A/d)$, where A is the surface area of one of the plates and d is the separation and ϵ is the permittivity of the medium between the plates. The two-dimensional TLM model, as developed in this work, assumes that the capacitor has depth Δl. The capacitor in Fig. 1 has $A = 0.01\Delta l$ m^2, $d = 0.005$ m, hence $C = 2\epsilon\Delta l$. This method is apparently similar to the method described in [1,2].

In the TLM model each node is replaced by an equivalent circuit. The method is derived from converting the incident (i – superscript) voltage to a reflected voltage (r – superscript) through each time-step $\delta t = \Delta l/c\sqrt{2}$, where c is the speed of electromagnetic radiation. In this section the mesh only encloses the space between the plates of the capacitor. Extended meshes are considered in Section 7.

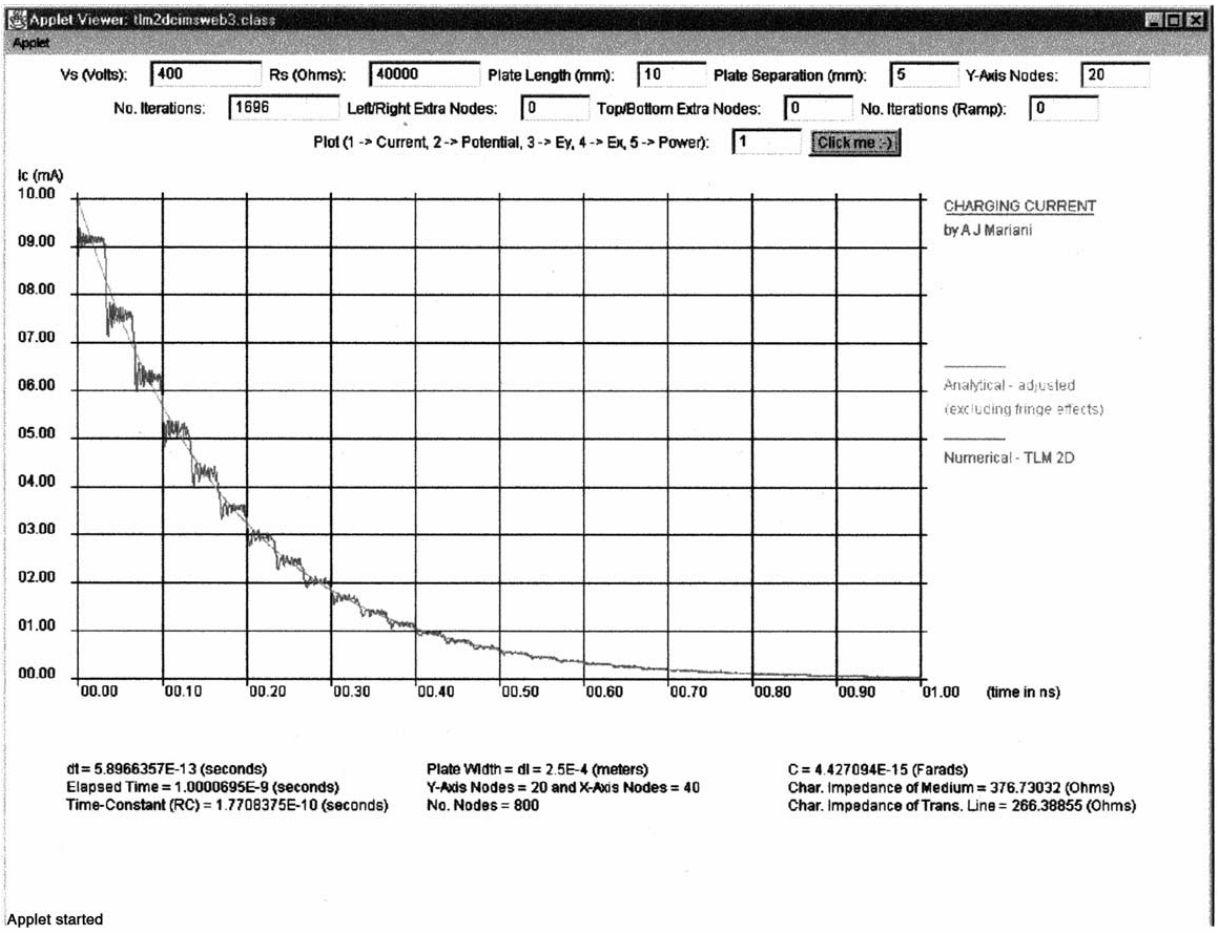

Fig. 6. Current in circuit for the 40×20 mesh.

3.1. Thevenin equivalent circuit

The port configuration surrounding each node in Fig. 1 is shown in more detail in Fig. 2. A voltage pulse incident on each open circuit termination is reflected, so that the total voltage at the termination is equal to twice the incident voltage. Hence an observer at each open circuit termination can replace it by the Thevenin equivalent circuit, where the voltage is twice the incident voltage and the impedance is Z_{TL}. The Thevenin equivalent circuit is shown in Fig. 3. The characteristic impedance of a TEM mode in air is $Z_{\mathrm{C}} = 120\pi$. The 2D TLM characteristic impedance is $Z_{\mathrm{TL}} = Z_{\mathrm{C}}/\sqrt{2}$.

3.2. Properties of the cell

If we consider the properties of the full equivalent circuit in Fig. 3 in the anticlockwise direction of the arrow,

$$V_{lm} = 2(V^{\mathrm{i}}_{1\,lm} + V^{\mathrm{i}}_{4\,lm} - V^{\mathrm{i}}_{2\,lm} - V^{\mathrm{i}}_{3\,lm}),$$

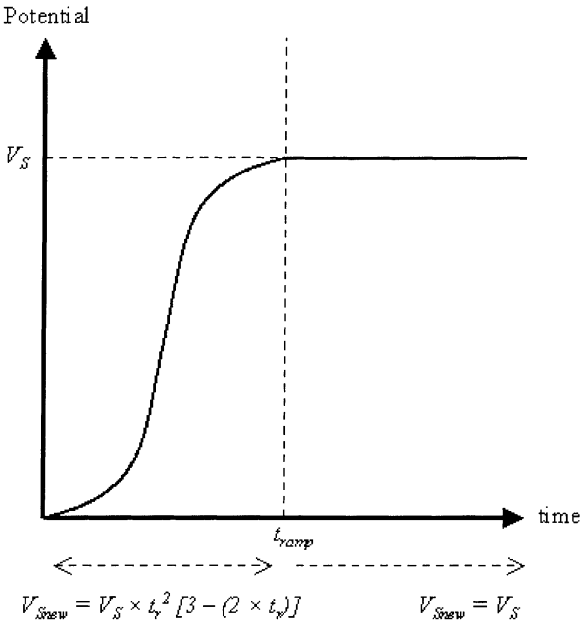

Fig. 7. The smooth switch-on.

$$Z_{lm} = 4Z_{\mathrm{TL}},$$

$$I_{lm} = \frac{V_{lm}}{Z_{lm}}.$$

The *lm* refers to the cell in the *l*th row and the *m*th column. V_{lm} is the potential of the full cell, Z_{lm} is the impedance and I_{lm} is the current.

The port voltage, the voltage across each side of Fig. 3, illustrated by the four arrows is given by:

$$V_1 = 2V^{\mathrm{i}}_{1\,lm} - I_{lm}Z_{\mathrm{TL}},$$

$$V_2 = 2V^{\mathrm{i}}_{2\,lm} - I_{lm}Z_{\mathrm{TL}},$$

$$V_3 = 2V^{\mathrm{i}}_{3\,lm} - I_{lm}Z_{\mathrm{TL}},$$

$$V_4 = 2V^{\mathrm{i}}_{4\,lm} - I_{lm}Z_{\mathrm{TL}}.$$

The reflected voltage is the port voltage less the incident voltage:

$$V^{\mathrm{r}}_{1\,lm} = V_1 - V^{\mathrm{i}}_{1\,lm},$$

$$V^{\mathrm{r}}_{2\,lm} = V_2 - V^{\mathrm{i}}_{2\,lm},$$

$$V^{\mathrm{r}}_{3\,lm} = V_3 - V^{\mathrm{i}}_{3\,lm},$$

$$V^{\mathrm{r}}_{4\,lm} = V_4 - V^{\mathrm{i}}_{4\,lm}.$$

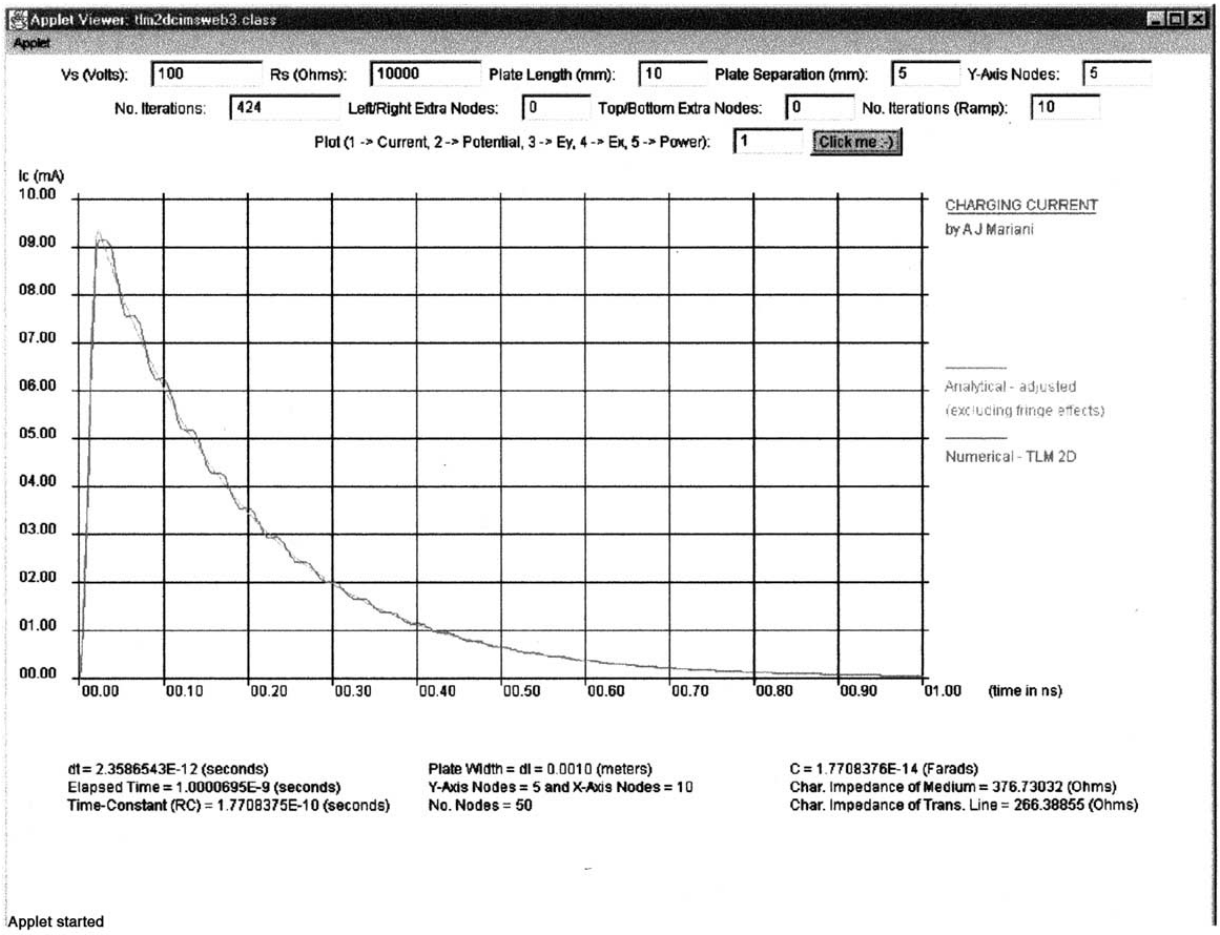

Fig. 8. Graph of current for smooth switch-on, $t_{\text{ramp}} = 10\Delta t$.

3.3. Updating

To complete the processes in the time-step, the reflected voltages are passed as incident voltages for use in the next time-step. The reflected voltages from neighbouring cells are passed as the new incident voltages:

$$V^{\text{i}}_{1\,lm} \leftarrow V^{\text{r}}_{3\,l,m-1},$$

$$V^{\text{i}}_{2\,lm} \leftarrow V^{\text{r}}_{4\,l-1,m},$$

$$V^{\text{i}}_{3\,lm} \leftarrow V^{\text{r}}_{1\,l,m+1},$$

$$V^{\text{i}}_{4\,lm} \leftarrow V^{\text{r}}_{2\,l+1,m}.$$

On the edges and corners of the domain the boundary condition must be applied. On the left- and right-hand sides of the mesh the boundary is open, a suitable condition must be placed on the

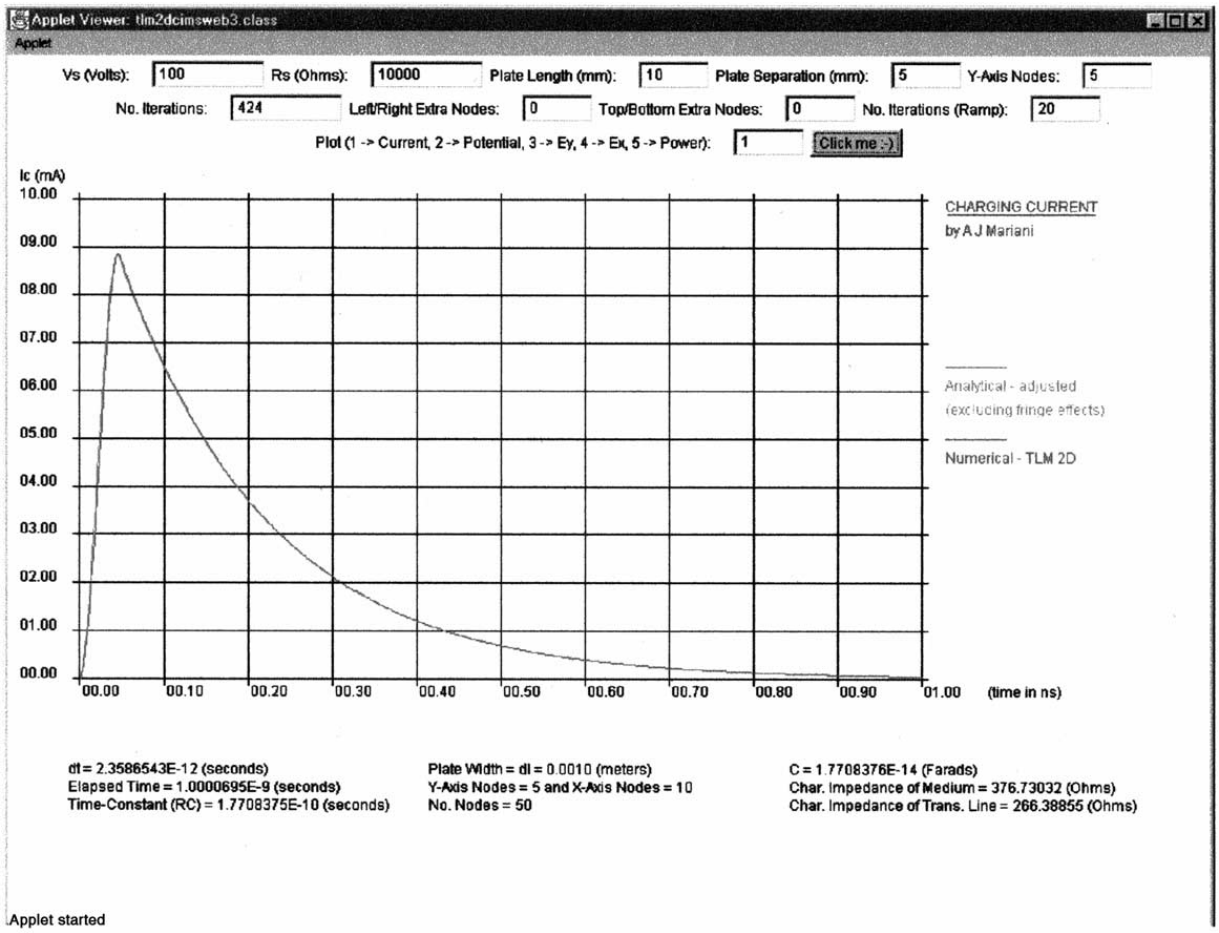

Fig. 9. Graph of current for smooth switch-on, $t_{\text{ramp}} = 20\Delta t$.

sides to model this. On the right side $l = 1$ so there is no $l - 1$ node leading to the second equation being replaced by

$$V^{\text{i}}_{2\,1m} \leftarrow \Gamma V^{\text{r}}_{4\,1,m},$$

where Γ is the reflection coefficient. Similarly at the left side ($l = L$):

$$V^{\text{i}}_{4\,Lm} \leftarrow \Gamma V^{\text{r}}_{2\,L,m}.$$

On the capacitor plates we need to impose a conduction boundary condition. On the top plate $m = 1$, hence the first equation is replaced by

$$V^{\text{i}}_{3\,l1} \leftarrow -V^{\text{r}}_{1\,l,1}.$$

Similarly for the bottom plate $m = M$, the third equation is replaced by

$$V^{\text{i}}_{1\,lM} \leftarrow -V^{\text{r}}_{3\,l,M}.$$

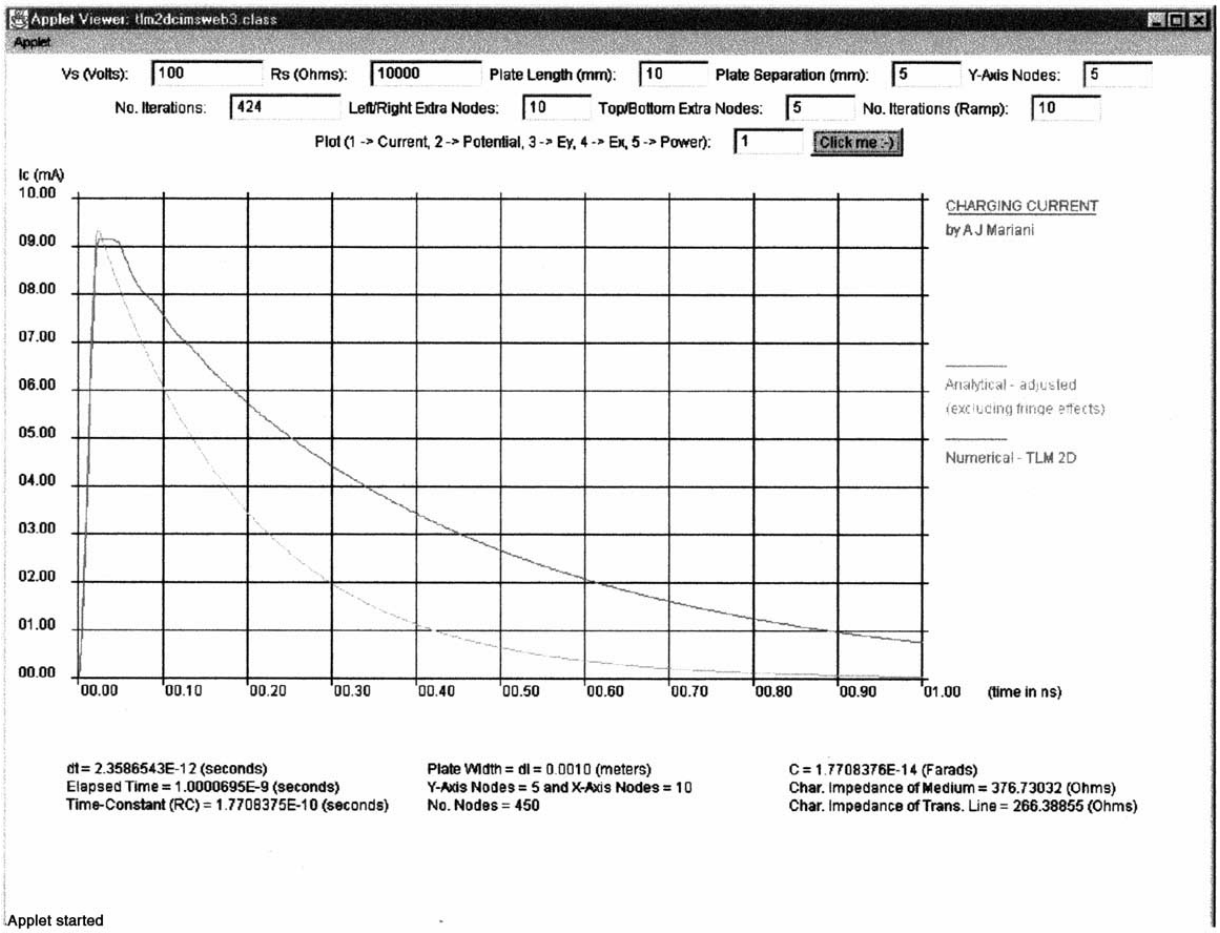

Fig. 10. Graph of current for smooth switch-on, $t_{\text{ramp}} = 10\Delta t$ and extended mesh and absorbing b.c.

4. Coupling the capacitor with the external circuit

As the capacitor charges the potential difference across it increases and this opposes the voltage of the source. The current in the circuit is informed by the charge on the capacitor and vice versa. Hence the distributed capacitor modelled by the TLM must be coupled to the other components of the circuit to complete the model.

The potential difference across the capacitor can be determined by finding the line integral of the electric field intensity along any line between the two contacts. Hence the most straightforward method for the capacitor considered in this work is the direct line between the contacts

$$V_X \leftarrow \sum_{m=1}^{m=M} \{V^{\mathrm{r}}_{2X+1,m} + V^{\mathrm{r}}_{4X,m}\},$$

where $l = X$ is the contact node (in the capacitor of Fig. 1, $X = L/2$).

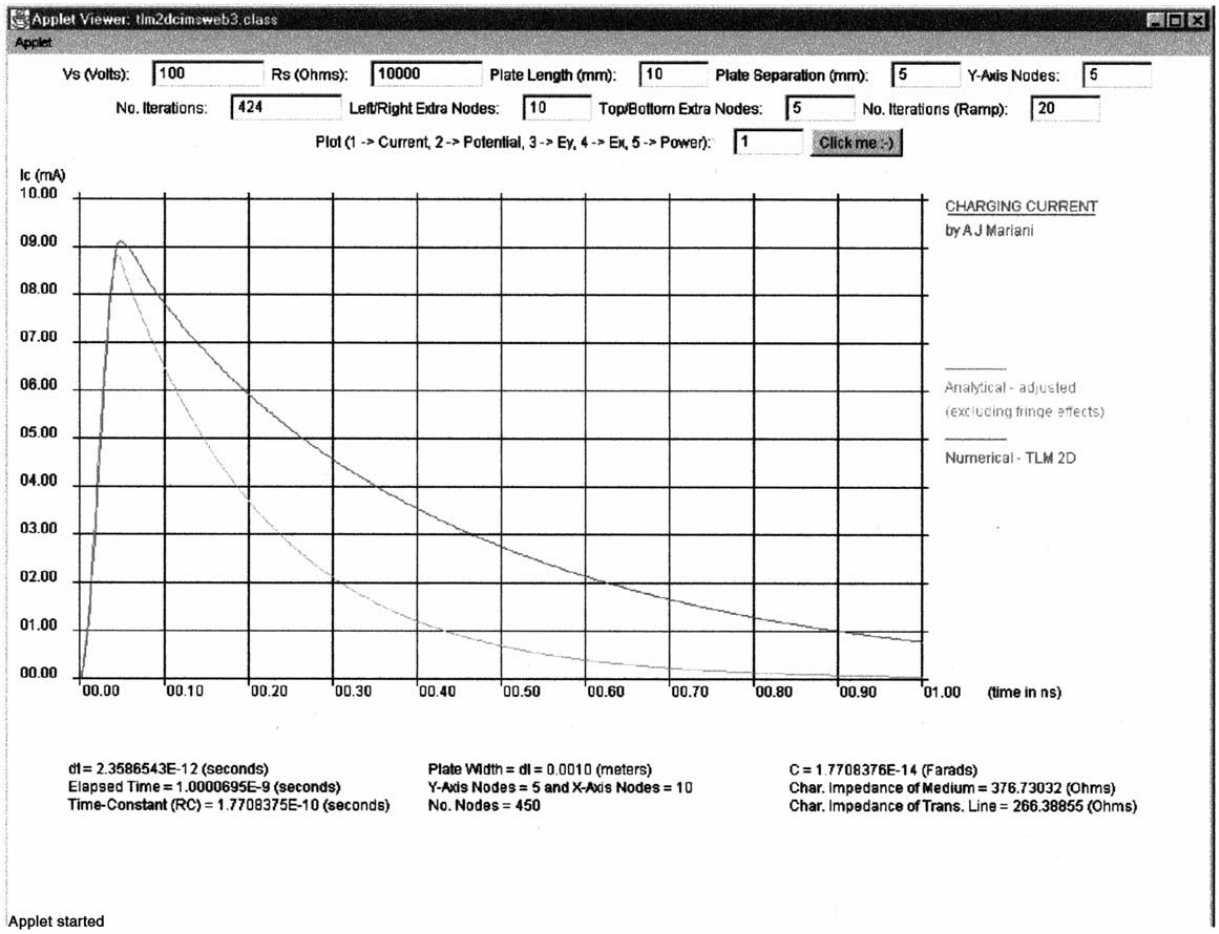

Fig. 11. Graph of current for smooth switch-on, $t_{\text{ramp}} = 20\Delta t$ and extended mesh and absorbing b.c.

The total impedance across the contacts is given by

$$Z_X \leftarrow \frac{1}{2} M Z_{\text{TL}}.$$

The current is equal to the effective voltage divided by the effective impedance of the circuit

$$I_X \leftarrow \frac{V_{\text{S}} - V_X}{R_{\text{S}} + Z_X}.$$

Finally a method is needed to inform the capacitor of the current flowing into it. In [1,2], the incident voltages in the cells between the contacts are modified as follows:

$$V^{\text{i}}_{4\,lm} \leftarrow V^{\text{i}}_{4\,lm} + \frac{1}{2} I_X Z_{\text{TL}}, \tag{3}$$

$$V^{\text{i}}_{2\,lm} \leftarrow V^{\text{i}}_{2\,lm} + \frac{1}{2} I_X Z_{\text{TL}}. \tag{4}$$

The updates of (3) and (4) in effect place current sources between the contacts of the capacitor and this technique will be termed the *current sources method.*

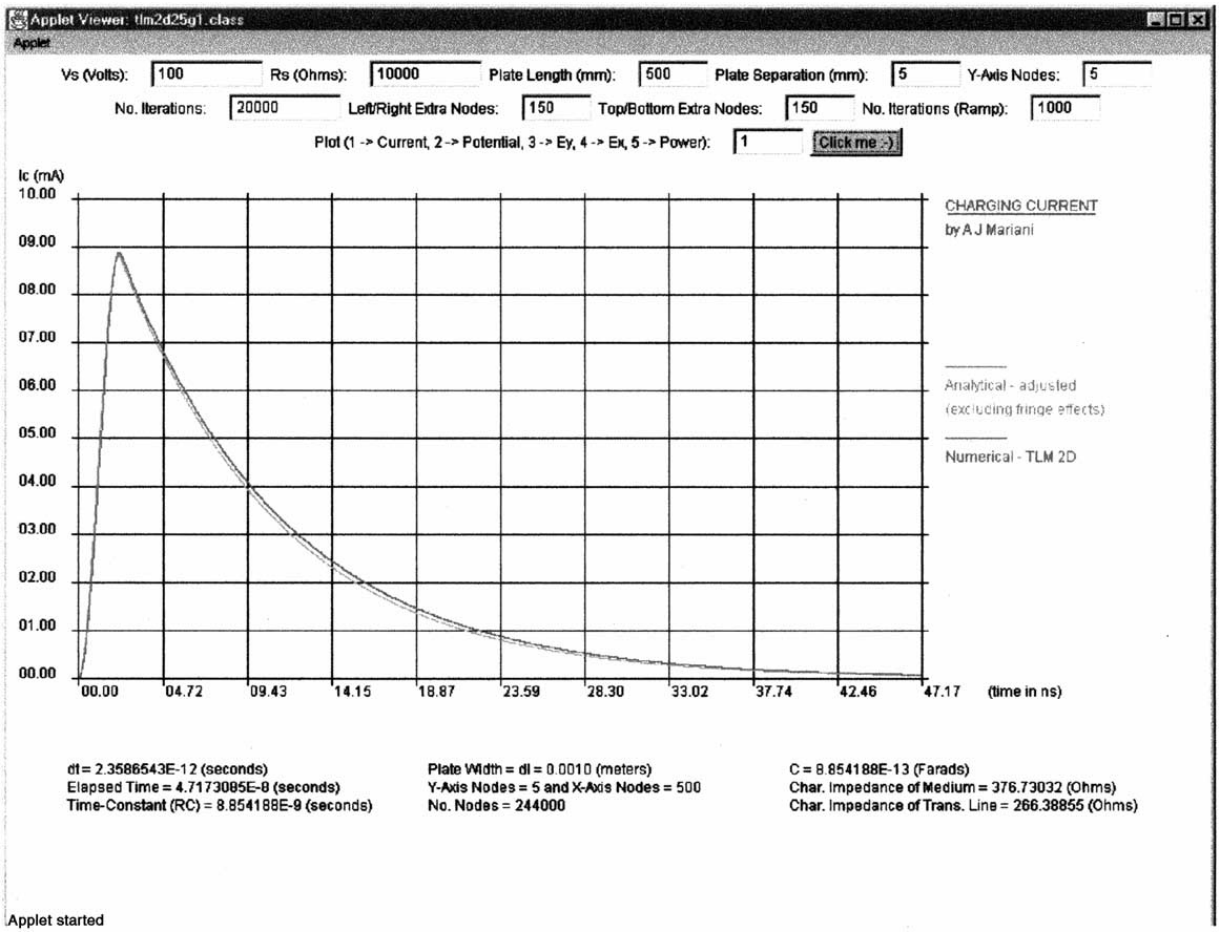

Fig. 12. Graph of current for smooth switch-on, $t_{\text{ramp}} = 10\Delta t$, extended mesh and absorbing b.c. for thin capacitor.

5. Implementation in Java

The TLM method described in the previous sections was developed in the Java programming language. Java is a relatively new language with a C-like syntax and it is available free from the world wide web site http://www.sun.com. One advantage of Java over many other programming languages is that it has added features such as graphics and a graphical user interface within the standard language. Hence an application containing such features will run equally well on all computers, whether they be PCs, Macs or Unix workstations.

Compiled Java codes are .class files and these may be developed as web pages. The user's browser interprets the codes and the user is able to interact with the web pages. The fact that a programmer can make applications immediately available to a world-wide audience is perhaps the most important advantage of Java.

The Java program is available via the web page http://www.electromagnetics.co.uk/tlm.htm. The conditions of the circuit such as source voltage and resistance, the length and separation of the capacitor plates may be chosen by the user. The conditions of the numerical simulation may also

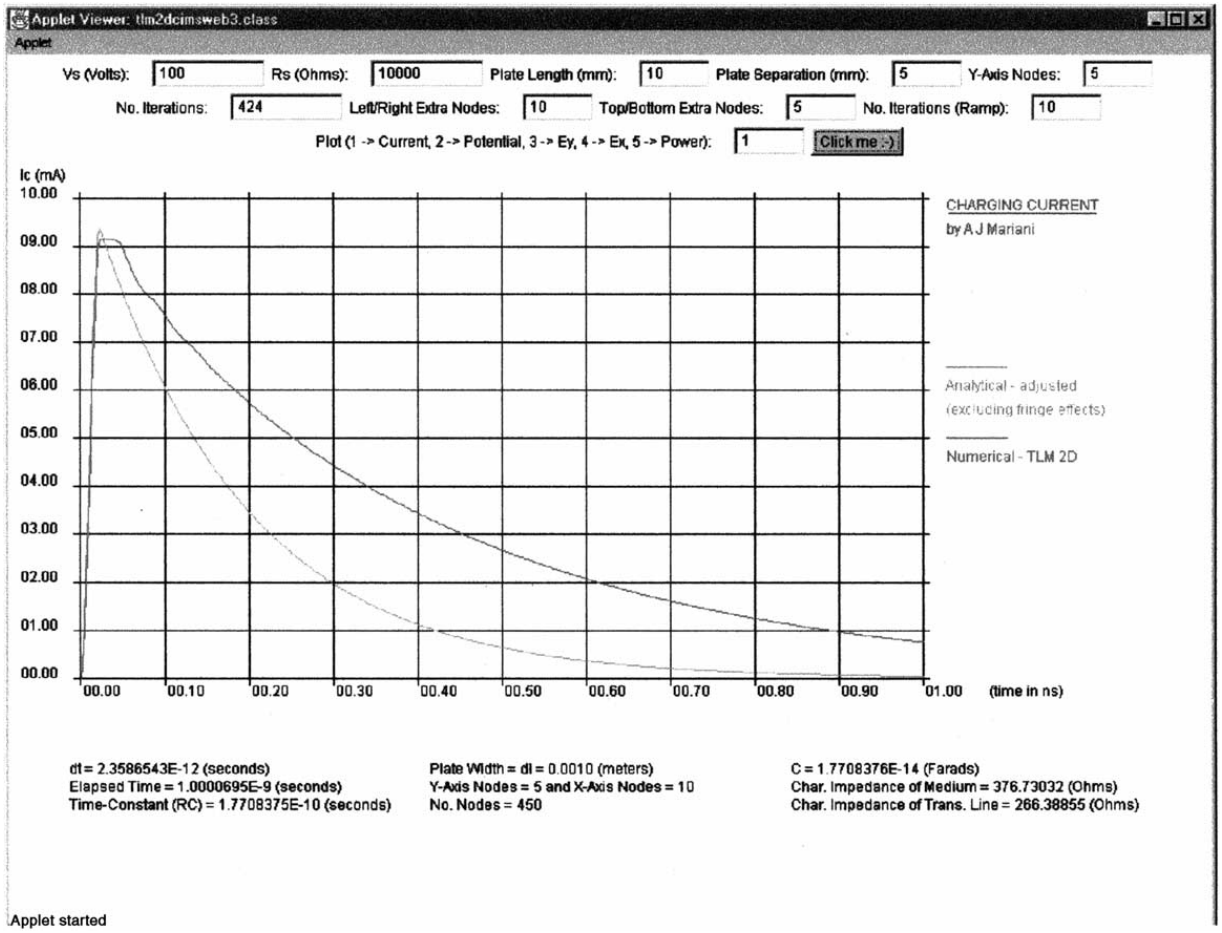

Fig. 13. Graph of current for smooth switch-on, $t_{\text{ramp}} = 10\Delta t$, extended mesh and $\Gamma = 1$.

be selected, such as the mesh size and the extent of the extended mesh, the number of time-steps and the boundary condition. The graph of the results of the computed and analytic current in the circuit is given on the screen. Typical results are given throughout the rest of this paper.

6. Initial numerical experiments and results

In this section the TLM method is applied in the same way as in [1] in order to verify the method. In this case the mesh covers the domain immediately between the capacitor plates only. Results from using finer meshes are also given.

6.1. Verifying the method

The TLM method implementing the example cited in [1] is run and using the same mesh. The reflection coefficient (Γ) at the ends of the capacitor is taken to be 1. The current in the circuit is shown in the graph of Fig. 4, where the time division is equal to 0.23×10^{-11}. The results show the exponentially decay curve but with a high degree of noise superimposed upon it.

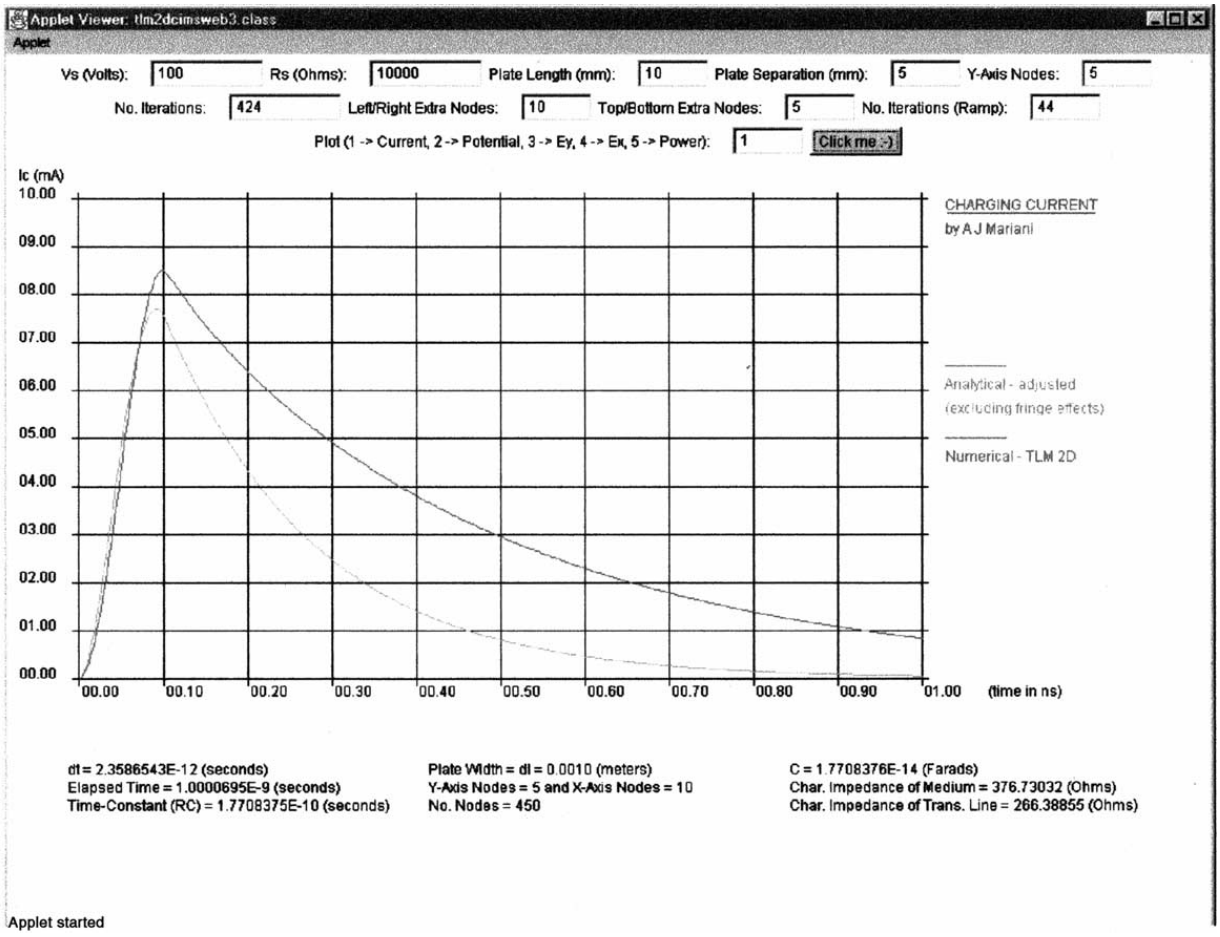

Fig. 14. Graph of current for smooth switch-on, $t_{\text{ramp}} = 20\Delta t$, extended mesh and $\Gamma = 1$.

6.2. Results using finer meshes

Finer computational meshes have been implemented in order to investigate whether such an approach would converge to the expected smooth decay curve. However the comparison is only useful if other conditions are altered, given the implicit assumption about the depth of the capacitor in the TLM method as it has been developed here.

For example when the mesh size was halved, this also led to the halving of the width of the capacitor (the capacitor is 1 cell deep in 2D TLM), so the capacitance C is halved. In order to normalise the results with respect to the previous results, R_S is doubled (to 20 kΩ) so that the analytic decay curve has same decay rate and V_S is doubled (V_S is 200 V). In order to have the same initial current as in the initial experiment, V_S also needs to be doubled. The results from using the 40×20 mesh are shown in Fig. 5. Doubling the mesh again ($R_S = 40$ kΩ and $V_S = 400$ V) gives the results in Fig. 6. The graphs in Figs. 5 and 6 show the appearance not only of the noise apparent in Fig. 4, but also a series of discrete steps superimposed upon the exponential decay.

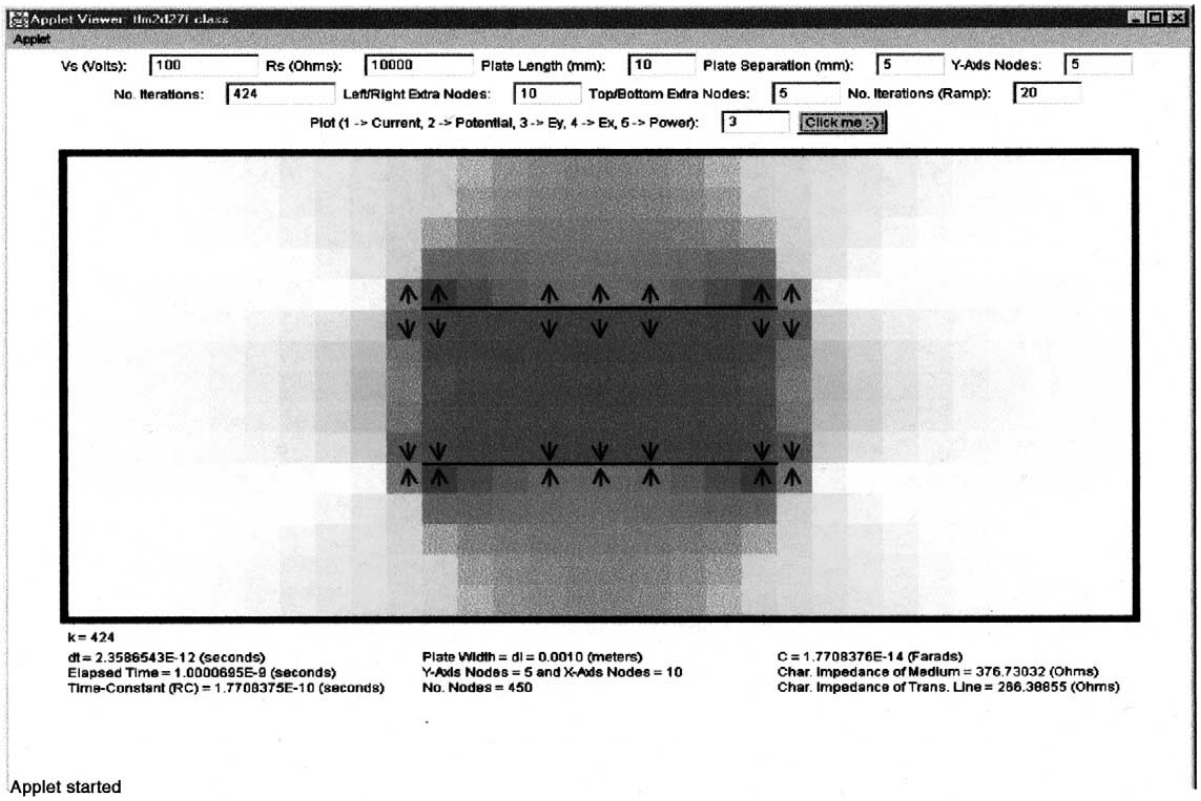

Fig. 15. Computed E_y for charged capacitor, extended mesh.

6.3. Discussion

The graph shown in Fig. 4 is very similar to Fig. 2 in [1], confirming the validity of the computer program. However, closer inspection of the results in Figs. 4–6 show several interesting features. Firstly, the computed graphs do not appear to converge to the expected smooth exponential decay curve as the mesh size is reduced.

Secondly, rather than converging to a smooth decay curve, the stepping that is apparent in Fig. 4 is enhanced as the mesh is refined giving a staircase solution with the expected solution passing through the centre of each step. It can be noted that there are three steps in the first 0.1 ns, hence each step takes approximately 0.033 ns. The propagation velocity of electromagnetic waves is approximately 3×10^8 m/s, hence this time translates to a distance of around 0.01 m or L, the width of the capacitor. Hence the duration of each step (t^*) is equal to time taken for a signal to pass from the centre to the edge of the capacitor and back again to the centre

$$t^* \approx \frac{L}{c},$$

where c is the velocity of electromagnetic waves in the dielectric.

The TLM solution is clearly also affected by noise. Later we will confirm that this results from the abrupt switch-on.

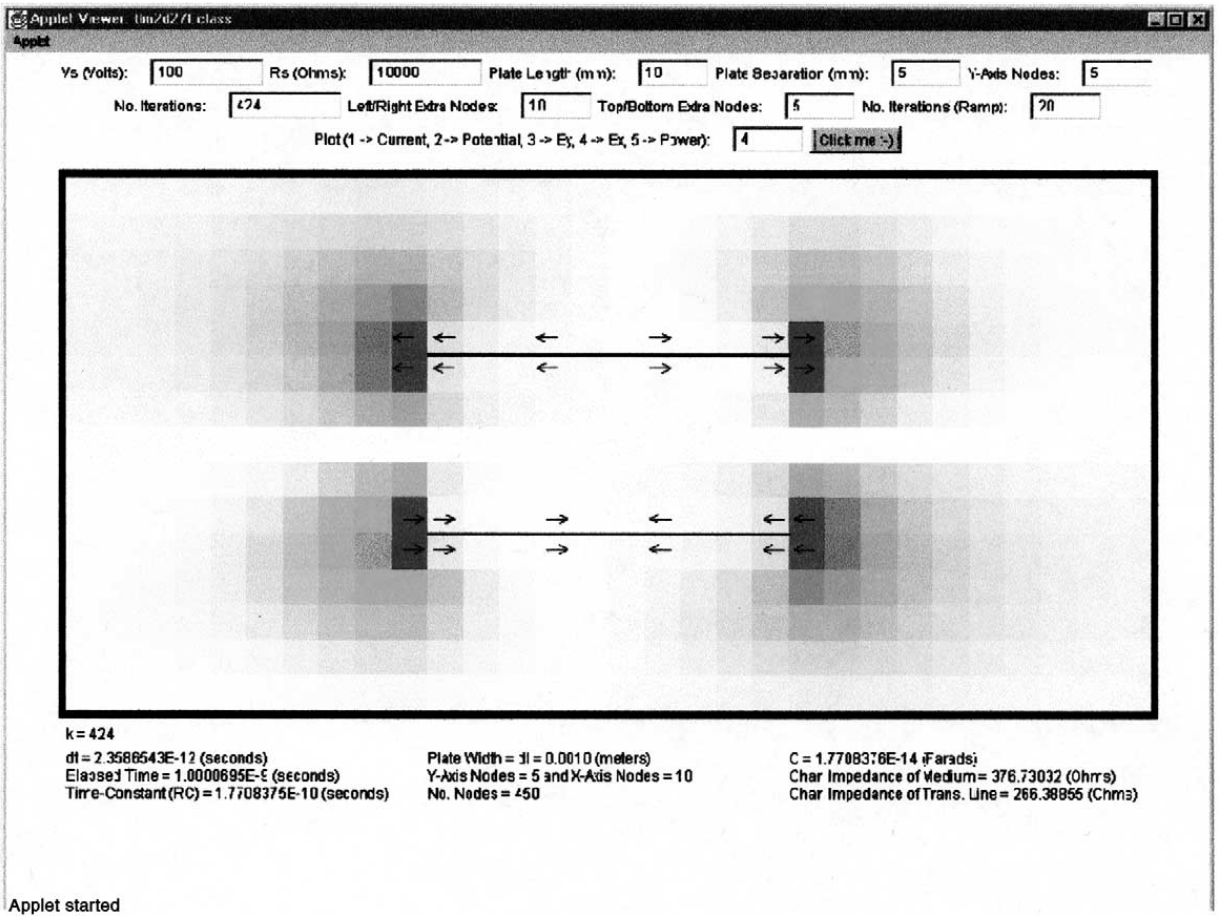

Fig. 16. Computed E_x for charged capacitor, extended mesh.

7. The solution for current ramps

Hitherto the electrical network has been excited by an abrupt switch-on from 0 to V_S at time $t = 0$. However, it is more realistic to utilise a voltage ramp of duration t_{ramp} for example. Let the time $[0, t_{ramp}]$ be known as the ramping time and let the voltage take the polynomial form in the period $[0, t_{ramp}]$:

$$V(t) = \left(\frac{t}{t_{ramp}}\right)^2 \left(3 - 2\frac{t}{t_{ramp}}\right) V_S \tag{5}$$

with $V(t) = V_S$ for $t > t_{ramp}$. The applied voltage curve is then the simplest polynomial form then ensures a continuous function with a continuous derivative (Fig. 7).

The analytic solution in $[0, t_{ramp})$ is given by Eq. (2). The remaining solution is obtained by delaying the decay (2) curve by half the ramping time for $t \geqslant t_{ramp}$

$$I(t) = \frac{V_S}{R_S} \exp\left(\frac{1}{R_S C}\left(\frac{t_{ramp}}{2} - t\right)\right) \quad \text{for } t \geqslant t_{ramp}.$$

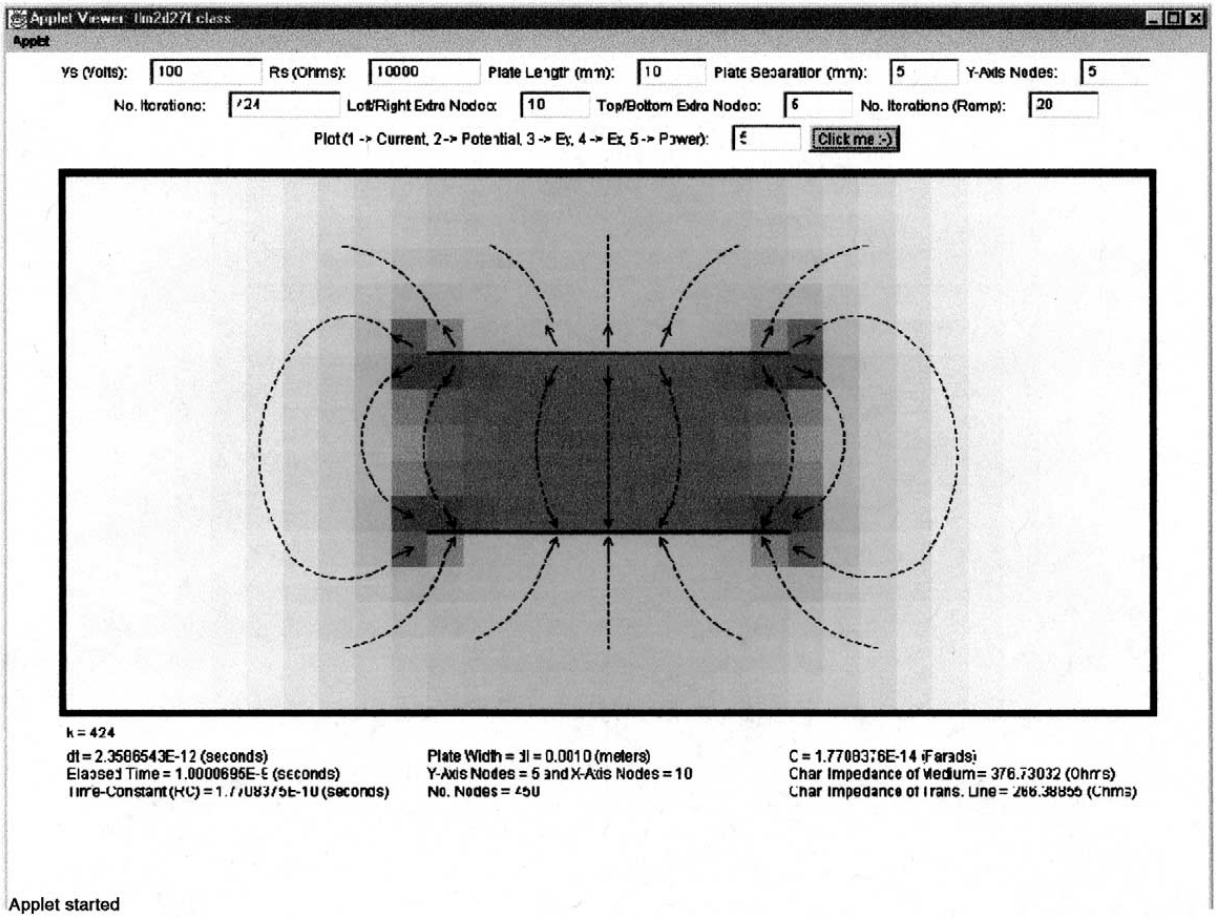

Fig. 17. Computed power for charged capacitor, extended mesh.

In Figs. 8 and 9 the test of Fig. 4 is re-run but with a smooth switch-on. In Fig. 8 $t_{\text{ramp}} = 10\Delta t$ and in Fig. 9 $T = 20\Delta t$ and the results are compared with an analytic solution given above. The results show that the noise has been eliminated by the smooth switch-on. If the ramping time t_{ramp} is larger than $t^*(= L/c)$, then the stepping is also eliminated (Fig. 9).

8. Extended mesh

In all of the tests presented above the TLM mesh has only covered the area between the plates of the capacitor. In this section results from extending the mesh beyond this are considered. The test calculations of Figs. 8 and 9 have been repeated and the results are presented in Figs. 10 and 11. Ramping times of $10\Delta t$ and $20\Delta t$ have been used. However the mesh is extended with five extra cells above and below the plates and 10 extra nodes to the left and right.

The results in Figs. 10 and 11 show a slower decay, because the complete electrical field including the fringe effects is now modelled. To demonstrate this, an extended mesh for a thin capacitor is employed and the result is shown in Fig. 12. For this the fringe field is small and the computed and analytic results show good agreement.

9. Reflection coefficient

Part of the problem of modelling the capacitor is the choice of reflection coefficient Γ. In the examples presented above when the mesh was not extended, the reflection coefficient was given the value $\Gamma = -1$ (short circuit) on the plate and $\Gamma = 1$ (open) on the sides of the capacitor. Any other value of Γ on the sides gave unsatisfactory results.

For the extended mesh in the previous section, in Figs. 10 and 11, the reflection coefficient was given the value $\Gamma = (\sqrt{2}-1)/(\sqrt{2}+1)$ corresponding to an absorbing or matched boundary condition. If an open circuit boundary condition is applied on the extended mesh ($\Gamma = 1$), but with other conditions kept the same, then the graphs in Figs. 13 and 14 are obtained, again ramping times of $10\Delta t$ and $20\Delta t$, respectively.

10. The electromagnetic field

So far results have been shown for the current in the circuit only. However, the main reason for modelling a distributed component is to obtain a detailed analysis of the electromagnetic field within it.

10.1. Extended mesh

Figs. 15–17 show colour plots of the electric field within and surrounding the capacitor using an extended mesh. The colour scheme ranges from dark cyan to light cyan in high negative to negative areas, then from yellow to red in positive areas. The figures illustrate E_x, E_y and the power $\sqrt{E_x^2 + E_y^2}$.

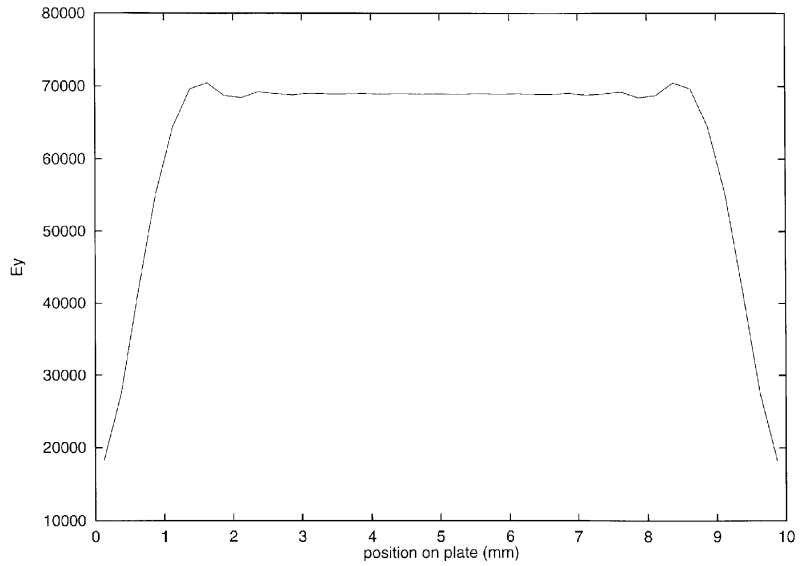

Fig. 18. E_y along central line of capacitor, non-extended mesh, charging in process.

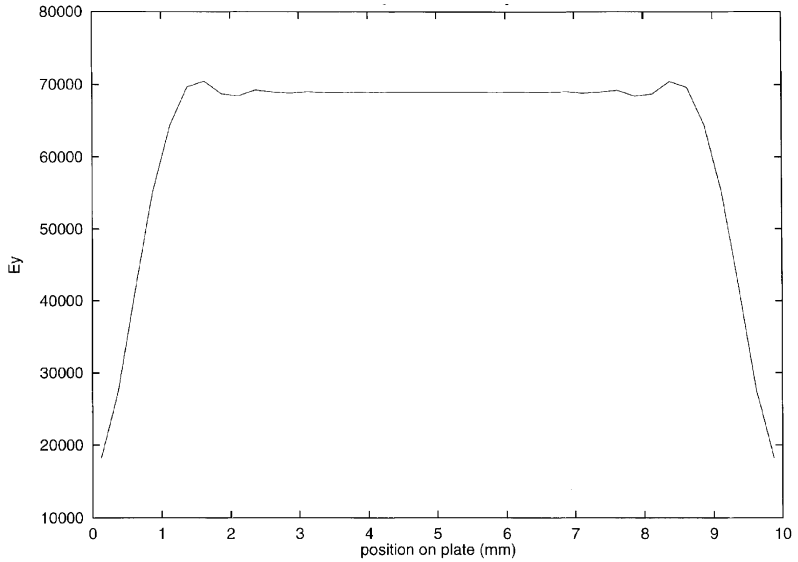

Fig. 19. E_y 1/4 way up line of capacitor, non-extended mesh, charging in process.

10.2. Non-extended mesh

Fig. 18 shows the electric field intensity E_y along the central horizontal line of the capacitor and Fig. 19 plots the same but one-quarter way up the capacitor. For these plots the mesh was 40×20, not extended, the data were taken after $30\Delta t$ with $t_{\text{ramp}} = 10\Delta t$. It can be observed that the two graphs are identical. Thus the electromagnetic field is one-dimensional within the capacitor for the non-extended mesh; the electric field intensity varies with x but not with y.

11. Conclusion

In this paper a distributed capacitor modelled by the TLM has been coupled with a lumped circuit using a current sources method. The initial results were verified through comparison with a published paper. It has been shown that the steps in the non-smooth decay curves which were initially produced in the present work and in [1] can be explained by wave reflections from the lateral ends of the capacitor. The noise can be attributed to the abrupt switch-on, which is equivalent to a numerical shock. A smoothed switch-on method was introduced and it was shown that this can remove both the noise and the stepping.

Results obtained with the mesh extending beyond the limits defined by the capacitor plates and the introduction of an absorbing boundary condition leads to a slower decay. The inclusion of the wider field in the TLM mesh results in an effective increase in capacitance.

Although the *current sources method* has enabled the coupling of distributed and lumped components to be realised for a simple capacitor geometry and connected circuit, and the results obtained when a steady state is reached seem to be acceptable, there are a number of concerns with this approach. Firstly, in reality, the electric circuit is connected to the capacitor plates only at the two points of contact. Thus a rigorous representation should not a priori interfere with

conditions within the capacitor dielectric. The *current sources method* is equivalent to placing the external circuit within the domain of the distributed component.

Secondly, the field for the non-extended mesh is predicted to be one-dimensional. In general the field should be two-dimensional and so this places some doubt on the validity of the computed electromagnetic field in general.

Thirdly, the capacitor in Fig. 1 is a relatively simple structure. It is clear that the most straightforward approach is to place the current sources between the contacts. However real engineering structures (e.g. capacitors, circuit breakers) are of a more complex spatial distribution. In such cases there are no clearly defined positions at which to place the current sources.

Acknowledgements

The authors would like to thank Dr. M.G. Kong of Loughbourough University for his advice on the work covered in this paper. Mrs. Mariani is funded by EPSRC and the National Grid Company. Dr. Kirkup acknowledges the support provided by EPSRC and ABB Power T&D.

References

[1] M. Al-Asadi, T.M. Benson, C. Christopoulos, Interfacing field problems modelled by TLM to lumped circuits, Electron. Lett. 30 (4) (1994).
[2] M. Al-Asadi, T.M. Benson, C. Christopoulos, A method for incorporating charged particle motion within 2-D TLM a field code, Int. J. Numer. Model.: Electronic Networks Devices Fields 9 (1996) 201–214.
[3] C. Christopoulos, The Transmission-line Modeling Method, Oxford University Press, Oxford, 1995.
[4] S.M. Kirkup, Capacitor Modelling by FD-TD, Proceedings of 6th IASTED Conference on Power and Energy Systems, 2001, pp. 178–183.
[5] S.M. Kirkup, Y. Huang, G.R. Jones, H.M. Love, DC Capacitor Simulation by an Integral Equation Method, Proceedings of the International Conference on Electromagnetics in Advanced Applications, ICEAA01, Torino, 2001, pp. 15–18.
[6] A.J. Mariani, Dynamic interaction of circuit breaker arcs with interconnected networks, CIMS Report, University of Liverpool, 1999, private communication.
[7] A. Taflove, Computational Electrodynamics: The Finite-difference Time-domain Method, Artech House Inc., Norwood, MA, USA, 1995.